The Issue of Morphology and Molecular Accessibility of Swollen Gel-Type Resins: An Integrated Inverse Steric Exclusion Chromatography−Electron Spin Resonance−NMR Approach

Angelo Antonio D'Archivio and Luciano Galantini

Dipartimento di Chimica, Ingegneria Chimica e Materiali, Universita' di L'Aquila, via Vetoio, 67010 Coppito, L'Aquila, Italy

Alberto Panatta and Enzo Tettamanti

Istituto Nazionale di Fisica della Materia (INFM), Dipartimento di Fisica, Universita' di L'Aquila, via Vetoio, 67010 Coppito, L'Aquila, Italy

Benedetto Corain*

Institut für Organische Chemie und Biochemie, TU München, Lichtenbergstrasse 4, 85747- Garching, Germany

Received: January 23, 1998; In Final Form: June 9, 1998

A number of microporous fairly hydrophilic poly(*N*,*N*-dimethylacrylamide-methylenebisacrylamide) (poly(DMAA-MBAA)) resins (cross-linking degree from 2 to 8%) have been examined with techniques that provide information on the structure on the nanometer scale and molecular accessibility of these materials in the swollen state. Electron spin resonance (ESR), pulsed-gradient-spin-echo nuclear magnetic resonance (PGSE−NMR) spectroscopies, and inverse steric exclusion chromatography (ISEC) gave consistent results in water, tetrahydrofuran (THF), and dichloromethane (DCM). The results are interpreted on the basis of physical models which fit reasonably the experimental data. The resulting equations between the translational diffusion coefficient of the solvent, the rotational correlation time of the spin-probe 2,2,6,6-tetramethyl-4-oxo-1-oxylpyperidine (TEMPONE) dispersed inside the swollen resins, and the polymer chain concentration appear to be promising tools in the design of macromolecular materials for chemical and catalytic applications.

Introduction

Gel-type resins are currently widely utilized as ion-exchangers,[1] as environmentally friendly acid catalysts, e.g., in the synthesis of bisphenol A,[2] and as enzyme supports in biocatalysis.[3] All of these applications are performed under solid−liquid conditions, i.e., in circumstances under which the resin polymer backbone may undergo extensive solvation (depending on the solvent-to-polymer affinity[4]) so that the whole of the resin polymer backbone is said to be "swollen" by the liquid medium.[2b]

Swelling implies the development of a certain degree of nanoporosity within the polymer network, which is not present in the dry state. The structure of these materials in the swollen state can be schematically depicted as a three-dimensional system of "meshes", which results from the entangling of cross-linked polymer chains. In view of the intrinsically inhomogeneous distribution[5] of the polymer chain concentration,[6] the actual size of the resulting meshes (in a given swelling medium) cannot be defined for a given polymer network, but is characterized in fact by a size distribution pattern. In all of the above-mentioned applications, the functional capabilities of microporous supports are chiefly conditioned by their molecular accessibility, namely by their ability to be crossed by reagents and products moving to and from the catalytically active sites. In this connection, chemical intuition predicts that the translational mobility of these species is controlled by the average polymer chain concentration, and, considering that the cavities defined by the polymer chains are nanometric in size, physics tells us that the diffusion rate of the molecules is decreased by (at least) a microviscosity effect.[7]

Despite the economic relevance and the obvious potentialities of gel-type resins as advanced materials for further catalytic applications,[8,9] and as finely designable supports for metal catalysis,[10] physicochemical investigations are relatively scanty[11] and certainly do not appear to be finalized to the specific design and optimization of catalytically relevant materials.

We have recently reported[11] on a promising example of a novel strategy aimed at correlating the information stemming from a rather complex and time demanding (although highly informative) technique, such as inverse steric exclusion chromatography (ISEC), with results offered by simple electron spin resonance (ESR) measurements performed on paramagnetic probes, characterized by well-known hydrodynamic radii, confined into the examined swollen resin. The two techniques, applied to lightly cross-linked poly(*N*,*N*-dimethylacrylamide-methylenebisacrylamide) (poly(DMAA-MBAA)) resins obtained upon γ-irradiation at −78 °C in mass, provide quite independent and complementary information on the investigated matrixes and a quantitative correlation between the rotational correlation time of the probe (τ provided by ESR) and the polymer chain

* To whom correspondence should be addressed. On leave of absence from Dipartimento di Chimica, Ingegneria Chimica e Materiali, via Vetoio, 67010 Coppito, L'Aquila, Italy and from Centro per lo Studio della Stabilità e Reattività dei Composti di Coordinazione, C.N.R., c/o Dipartimento di Chimica Inorganica Metallorganica e Analitica, via Marzolo 1, 35131 Padova, Italy.

S1089-5647(98)00855-4 CCC: $15.00
Published on Web 08/11/1998

TABLE 1: Synthetic Data on Resins M2, M4, M6, M8

resin	C%	H%	N%	ncld[c]	yield %
M2	60.61[a]	9.04	14.32	2.0	87
	61.92[b]	9.56	14.53		
M4	60.09	8.92	14.33	3.9	94
	59.49	9.38	13.50		
M6	59.93	8.84	14.48	6.0	99
	59.92	9.43	13.85		
M8	60.04	8.80	14.67	8.1	96
	59.83	9.41	14.00		

[a] Theoretical for 100% polymerization yield. [b] Experimental. [c] Nominal cross-linking degree.

concentration c_c (see below) (provided by ISEC).[11] Consequently, a simple ESR measurement provides direct nanostructural (textural) information.

We report now on a more sophisticated analysis which involves also pulsed-gradient-spin-echo (PGSE)−NMR spectroscopy, which provides direct information on the translational mobility of a molecule in a given liquid phase.[12] The simplest case is a monocomponent liquid phase in the bulk state or confined inside a porous medium, which reduces the solvent mobility, and the final datum stemming from this analysis is the self-diffusion coefficient D.[12b] We will show that the three totally independent techniques provide a valuable integrated evaluation of morphology on the nanometer scale and molecular accessibility of the investigated materials.

Results and Discussion

Four gel-type resins characterized by nominal cross-linking degree (% mol) equal to about 2 (**M2**), 4 (**M4**), 6 (**M6**), and 8 (**M8**) are obtained upon γ-irradiation of the required DMAA-MBAA homogeneous mixture, at room temperature, with essentially quantitative yield (Table 1). In this respect, irradiation at room temperature and not at −78 °C,[11] makes no detectable difference.

In our previous paper,[11] we succeeded in accounting for the experimental relationship between the rotational mobility of 2,2,6,6-tetramethyl-4-oxo-1-oxyl-pyperidine (TEMPONE) inside gel-type resins quite similar to M2−M8, and their nanoporosity on the basis of a simple Stokes−Einstein approach to solvent viscosity and the assumption that the swollen polymer network is in fact a relatively concentrated solution of polymer chains. We will see here that this model still holds for the rotational mobility vs *weighed average polymer chain concentration*, $\langle c_c \rangle$, (see below) relationship. However, we anticipate that the model only partially rationalizes the clear experimental relationship between solvent diffusion coefficient and $\langle c_c \rangle$ as well as the clear relationship between rotational mobility of TEMPONE and translational mobility of the confined solvent.

ISEC Characterization of Resins M2−M8. ISEC is a version of the well-known and practiced size exclusion chromatography, which does not aim at the analysis or separation of analytes of expected different sizes, but, on the contrary, aims at defining the morphology on the nanometer scale of a given gel-type matrix on the basis of its behavior toward analytes of well-defined size (hydrodynamic radii). ISEC is particularly suited for analyzing microporous resins under operational conditions, i.e., in their swollen state. On the basis of Ogston's model[13] which considers polymer chains as cylindrical, randomly oriented rigid rods characterized by a realistic diameter, and after the methodological improvement introduced recently by Jeřàbek,[6] ISEC analysis provides for any gel-type resin (a) its gel volume as seen by the molecular probes employed, (b) the internal distribution of its domains characterized by given polymer densities, and (c) its $\langle c_c \rangle$ value, a figure which provides a sort of picture "in negative" of the nanoporosity of the polymer network. $\langle c_c \rangle$, being the length of the polymer chains in a unit volume, is expressed as nm/nm^3 = nm^{-2}. The direct experimental result of an ISEC test is the retention volume referred to a given probe, which is adequately retained by a column filled with the investigated resin, swollen by the solvent of choice. In this work we chose water and tetrahydrofuran (THF). The conceptual (and operational) passage from the retention volumes to the morphological information (Figure 1) occurs upon assuming that the total gel volume possessed by the sample is built up with five discrete fractions (domains) of polymer mass each characterized by its polymer chain concentration c_c (0.1, 0.2, 0.5, 1.0, and 2.0 nm^{-2}, respectively) and volume V (cm^3/g). The value 0.4 nm is chosen as a reasonable diameter of the polymer chains.

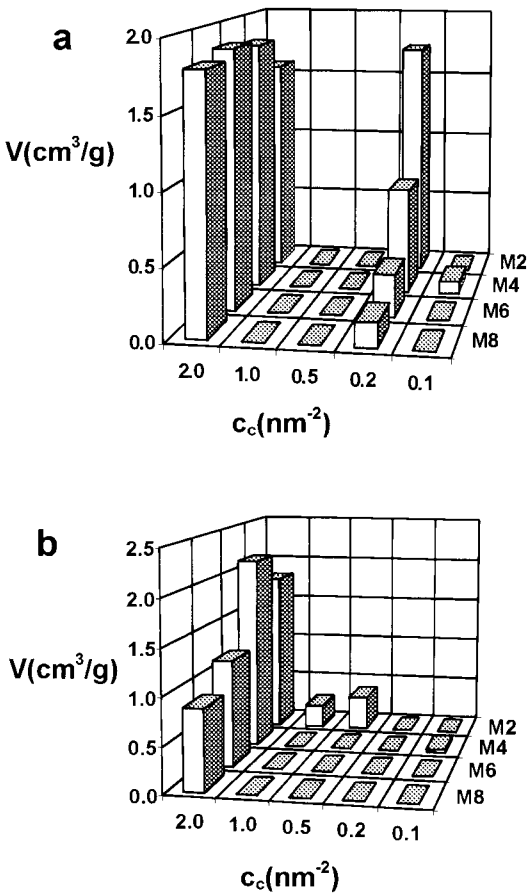

Figure 1. Volume distributions of variously dense polymer fractions in the resins **M2**−**M8**, as determined by ISEC in (a) water and (b) THF.

A strong criterion of reliability of ISEC conclusions is the agreement, for any employed swelling agent, between $\sum V_i$ (V_i = estimated volume of the i-th fraction of polymer mass) and the experimental V_g (V_g = determined volume of the total gel-type polymer mass) measured by means of a simple and reliable chromatographic experiment.[6]

Inspection of Table 2 reveals that, in this connection, the results referring to water are quite different from those referring to THF.

Thus, in water $\sum V_i$ compares well with V_g, but this is the case only for the less cross-linked resins in THF. Interestingly, in THF $\sum V_i$ is definitely lower than V_g for **M6** and **M8**, i.e.,

TABLE 2: Average Polymer Chain Concentrations ($\langle c_c \rangle$ (nm^{-2})) and Calculated ($\sum V_i$ (cm^3/g)) and Experimental (V_g (cm^3/g)) Values of the Total Gel Volumes of Matrices M2−M8 in Water and in THF

	water			THF		
resin	$\sum V_i$	V_g	$\langle c_c \rangle^a$	$\sum V_i$	V_g	$\langle c_c \rangle$
M2	3.32	3.12	1.06	2.44	2.57	1.67
M4	2.66	2.43	1.43	2.17	2.26	1.97
M6	2.16	1.97	1.75	1.16	2.25	2.00
M8	1.97	1.72	1.84	0.86	2.21	2.00

[a] $\langle c_c \rangle = \sum V_i c_{ci} / \sum V_i$.

TABLE 3: Observed Rotational Correlation Time, τ (ps), and Isotropic ^{14}N Hyperfine Splitting Constant, a_N (G),[a] Values for Resins M2−M8 After Swelling with Water, THF, and DCM

resin	water τ (ps), a_N (G)	THF τ (ps), a_N (G)	DCM τ (ps), a_N (G)
bulk solution	52, 15.87	41, 14.39	21, 14.60
M2	123, 15.77	488, 14.55	58, 14.60
M4	174, 15.73	658, 14.55	87, 14.61
M6	251, 15.71	721, 14.53	139, 14.63
M8	300, 15.67	861, 14.54	194, 14.63

[a] a_N values are given to ±0.04 G.

the molecular probes do "see" a lower fraction of the gel volumes owing to a polymer chain density evidently larger than 2.0 nm^{-2}. These last domains exhibit such a reduced porosity to be practically impenetrable by even small molecular probes.

Figures 1a and b illustrate pictorially the observations numerically expressed by the data in Table 2 and add further information. Thus, in water, the less cross-linked resin **M2** is characterized by two major gel domains with 2.0 and 0.2 nm^{-2} c_c values (total gel volume = 3.32 cm^3/g). The increase of cross-linking degree (paralleled by an increase of $\langle c_c \rangle$ from 1.06 to 1.84 cm^3/g) is accompanied by a gradual decrease of the absolute and relative contribution of the less dense domains (c_c = 0.2 cm^3/g) so that for **M8** the more dense domains are overwhelming the less dense domains. In THF, the data reveal that only denser domains are seen by the molecular probes utilized by the technique and that only for **M2** are relatively less dense (1.0 and 0.5 nm^{-2}) domains detected by ISEC probes. Thus, as a general comment to ISEC data, it can be observed that water swells effectively the polymer network causing an appreciable bulk expanded volume, part of which is characterized by lower chain density volumes; THF swells much less these gel-type resins which in fact are made predominantly (**M2**) and totally (**M4**−**M8**) by denser domains.

ESR Characterization of Resins M2−M8. In addition to water and THF, we considered also dichloromethane (DCM), a medium for which no ISEC data are available. After resins **M2**−**M8** were swelled with a 10^{-4} M solution of TEMPONE, the ESR spectrum of the paramagnetic reporter appeared to be uncomplicated[11] and its molecular motion was in the typical fast rotational region. The relevant τ values and the isotropic ^{14}N hyperfine splitting constants, a_N, (defined as one-half of the separation between +1 and −1 lines) are collected in Table 3. a_N, which reflects the local polarity experienced by the spin-probe, is practically not dependent on $\langle c_c \rangle$ in DCM- and THF-swollen resins, whereas it slightly decreases with the increasing of $\langle c_c \rangle$ in water. Thus, the local polarity at the probe site is not affected significantly by the polymer fraction, suggesting negligible or weak interactions between the spin-probe and the polymer network, which supports the hypothesis that the rotational diffusion is mainly controlled by the microviscosity of the confined solvent.

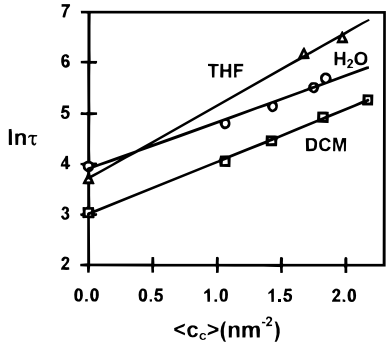

Figure 2. Dependence of rotational correlation times of TEMPONE (τ (ps)) on average polymer chain concentrations ($\langle c_c \rangle$) inside swollen **M2**−**M8** resins.

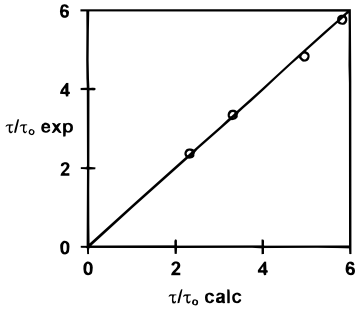

Figure 3. Graphical comparison between calculated and experimental relative rotational correlation times (τ/τ_0) of TEMPONE for resins **M2**−**M8** in water.

The ESR analysis reveals a relatively good rotational mobility of the spin-probe in all swelling media employed, even for **M6** and **M8** in THF.

The increase of $\langle c_c \rangle$ is always paralleled by an increase of τ, with τ values being definitely larger in THF in logical agreement with the ISEC results which predict higher $\langle c_c \rangle$ and, therefore, smaller nanoporosity. The plots of ln τ vs $\langle c_c \rangle$ are remarkably linear (Figure 2) for all swelling agents ($\langle c_c \rangle$ values for DCM are estimated figures stemming from PGSE−NMR results, see below).

ESR data collected in water are quantitatively correlated with the ISEC information utilizing the previously developed model:[11]

$$\tau/\tau_0 = \sum [K_i V_i A^{c_{ci}} / \sum K_i V_i] \qquad (1)$$

where τ_0 is the rotational correlation time of TEMPONE in the free solution and K_i is the Ogston's equilibrium distribution coefficient between the liquid phase and the *i*-th fraction of polymer.[11] Using the value 0.32 nm for the molecular radius of TEMPONE, the optimal value 2.80 for the adjustable parameter A is calculated.[11]

The excellent fitting between experimental and calculated values of τ/τ_0 is shown in Figure 3. Consequently, the quantitative correlation between the ISEC outputs and the ESR outputs is confirmed in water[11] and clearly observed in THF and DCM. Therefore, these new observations lend further credit to the major conclusions of ref 11.

PGSE−NMR Characterization of Resins M2−M8. PGSE ^1H NMR spectroscopy provides fine information on the translational mobility of proton-bearing solvents confined in nanoscopic volumes.[12] PGSE−NMR measurements were performed on water-, THF-, and DCM-swollen resins. The self-diffusion coefficients of water and DCM at 25 °C and activation energies of the diffusion process E_a calculated from Arrhenius

TABLE 4: Self-Diffusion Coefficients (D) and Activation Energies (E_a) Determined in Water and DCM Inside Resins M2−M8

	water		DCM	
resin	$D\cdot10^6$ (cm^2/s)	E_a (kcal/mol)	$D\cdot10^6$ (cm^2/s)	E_a (kcal/mol)
bulk solution	23.0	4.29	34.3	2.32
M2	14.5	5.16	16.7	2.25
M4	10.8	4.95	13.1	2.34
M6	8.6	5.28	10.4	2.90
M8	7.3	5.38	8.8	3.16

plots are shown in Table 4. From the measured self-diffusion coefficients the root-mean-square diffusion displacement of a solvent molecule over the duration of the experiment can be estimated. This displacement is given by

$$X_{rms} = (2Dt')^{1/2} \quad (2)$$

where t' is the time between the preparation pulse and the echo. For $D = 1.67 \times 10^{-5}$ cm^2/s, which is the largest measured for the solvents in the beds, and the typical $t' = 20$ ms, we obtain $X_{rms} = 8.2$ μm. This distance is much smaller than the diameter of the beads, which in the shrunk state is about 200 μm. This means that over the time of the experiment much of the solvent does not escape from the bead, and the measurement truly reflects the translational diffusion within the polymer network.

PGSE−NMR analysis in water and DCM shows a reduction of solvent diffusion rate which parallels the reduction of rotational mobility of TEMPONE and the increase of polymer chain concentration. The activation energy of the diffusion process does not depend significantly on $\langle c_c \rangle$, thus showing that the role of the polymer chains is that of inert "obstacles". Consequently, the reduction of D is in fact the result of a nanocavity effect just like that producing the reduction of rotational mobility[14] or of the increase of the path length due to the tortuosity of the path itself.

In THF-swollen resins, at room temperature, the echo signal is very low, especially in the more cross-linked resins, and the parameter D cannot be measured accurately. Apparently, the hindrance to translational mobility caused by the higher $\langle c_c \rangle$ (see above) makes so efficient the transversal relaxation of the magnetization that the echo amplitude is almost undetectable. This hypothesis is confirmed by the observed increase of the echo amplitude with increasing temperature and reflects the poorer swelling ability of THF compared with water and DCM (as it is raised in evidence by ISEC characterization).

Correlation Among ISEC, ESR, and PGSE−NMR Data. On the basis of the classical hydrodynamic theory of diffusion, a relationship between D and $\langle c_c \rangle$ can be predicted. As shown in ref 11 for the rotational diffusion, we can ascribe the reduction of the self-diffusion coefficient of the confined solvent to the increase of viscosity at the nanometric scale, η. Thus, from the combination of the Stokes−Einstein equation for translational diffusion, $D = kT/6\pi\eta r$, with $\eta = \eta_0 \cdot \exp(\nu\Phi)$, we get

$$\ln D = \ln D_0 - \nu\Phi \quad (3)$$

where D_0 is the self-diffusion coefficient of the pure solvent, Φ is the volume fraction of polymer chains, and ν is an adjustable parameter. If we refer to a resin according to the Ogston's model with polymer chains considered as cylindrical rods of radius r_c and characterized by a chain density $\langle c_c \rangle$,

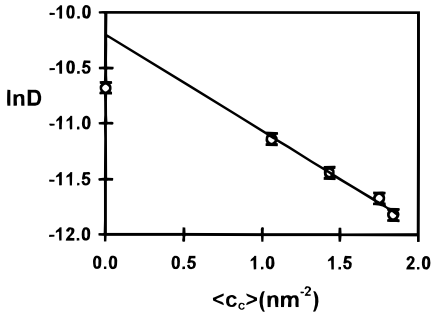

Figure 4. Dependence of self-diffusion coefficients (D (cm^2/s)) of water on average polymer chain concentrations ($\langle c_c \rangle$) for resins **M2**−**M8** in water.

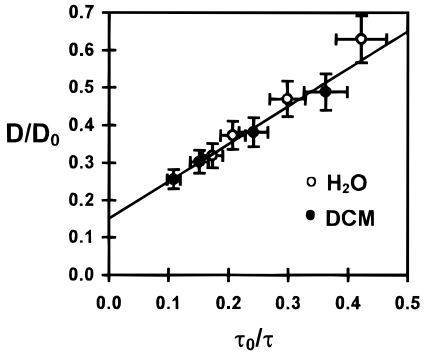

Figure 5. Dependence of relative self-diffusion coefficients of the solvent (D/D_0) on the reciprocal of relative rotational correlation times (τ_0/τ) of TEMPONE for water- and DCM-swollen **M2**−**M8** resins.

$\Phi = \pi r_c^2 \langle c_c \rangle$, and the relationship

$$\ln D = \ln D_0 - \nu\pi r_c^2 \langle c_c \rangle \quad (4)$$

is obtained.

The experimental plot of ln D vs $\langle c_c \rangle$ for **M2**−**M8** water-swollen resins is shown in Figure 4 and the good linear fitting of the data referring to the swollen matrixes is observed.

However, the D_0 value extrapolated from the plot ($3.72\ 10^{-5}$ $cm^2\ s^{-1}$) is somewhat higher than the measured value ($2.30\ 10^{-5}$ $cm^2\ s^{-1}$). Despite this disagreement, if we assume that both the solvent and TEMPONE molecules experience similarly the nanoviscosity of the medium, we expect to relate D with τ. Thus, if we combine the Stokes−Einstein equations for translational and rotational diffusion $D = kT/6\pi\eta r$ and $\tau = 4\pi a^3\eta/3kT$, respectively, the relationship

$$D/D_0 = \tau_0/\tau \quad (5)$$

is predicted.

In fact, the experimental data collected in water- and DCM-swollen resins reveal that D/D_0 results are a linear function of τ_0/τ in these two media, but the intercept is definitely different from zero and positive (Figure 5).

The experimental equation connecting D/D_0 with τ_0/τ becomes

$$D/D_0 = \tau_0/\tau + 0.15 \quad (6)$$

Upon combining this equation with $\ln \tau = \ln \tau_0 + \nu\pi r_c^2 \langle c_c \rangle$,[11a] the following equation is obtained for water and DCM:

$$\ln(D/D_0 - 0.15) = -\nu\pi r_c^2 \langle c_c \rangle \quad (7)$$

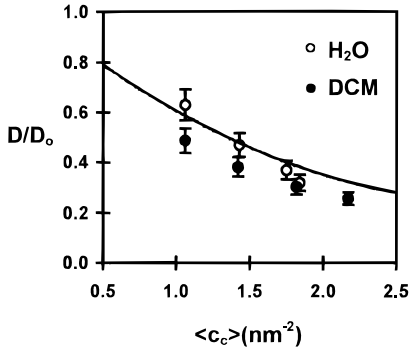

Figure 6. Dependence of relative self-diffusion coefficients (D/D_0) of water and DCM on average polymer chain concentrations ($\langle c_c \rangle$) for **M2**−**M8** resins. The continuous line is calculated from the Mackie and Meares equation (see text).

Upon calculating $\langle c_c \rangle$ in DCM from this relationship, the values 1.06, 1.42, 1.82, and 2.17 nm^{-2} for **M2**, **M4**, **M6**, and **M8**, respectively, are obtained. Figure 2 shows a remarkable linear correlation between ln τ and the so-determined $\langle c_c \rangle$ values and a substantial parallelism between the data obtained in water and DCM. In fact, this result implies the constancy of ν in the investigated solvents.

Another evaluation of the experimental relationship between ISEC and PGSE−NMR data as referred to classic hydrodynamic models can be put forward on the basis of the Mackie and Meares equation.[15] These authors developed in the 1950's a relationship between the diffusion coefficient of a given solvent which moves in the presence of impenetrable obstacles characterized by comparable size:

$$D/D_0 = (1 - \phi)^2/(1 + \phi)^2 \qquad (8)$$

where ϕ is the fraction of sites occupied by these obstacles. If we accept that the fraction of impenetrable sites can be replaced by the volumetric fraction of the impenetrable rods proposed in Ogston's model as conceptual tools for depicting the macromolecular chains, ϕ can be reasonably replaced by Φ. Therefore, by combining this last equation with the equation $\Phi = \pi r_c^2 \langle c_c \rangle$ (Ogston's model), the following relationship connecting D with $\langle c_c \rangle$ is obtained:

$$D/D_0 = (1 - \pi r_c^2 \langle c_c \rangle)^2/(1 + \pi r_c^2 \langle c_c \rangle)^2 \qquad (9)$$

Figure 6 illustrates that the experimental fittings are reasonable.

This observation is another good test for proving the quantitative correlation between ISEC and NMR data.

Experimental Section

Materials. DMAA (Aldrich), MBAA (Janssen), and TEMPONE (Fluka), and solvents (Carlo Erba) were used as received. THF was distilled over Na prior to use.

Synthesis of the Resins M2−M8. The resins were synthesized at 298 K by exposure of the comonomer mixtures to the γ-rays from a ^{60}Co source for 24 h (total dose: 1.8 Mrad). The resins were obtained as cylindrical rods, which spontaneously crumbled into millimeter-sized particles upon standing in methanol. After crumbling had apparently stopped, the resins were repeatedly washed with methanol, acetone, and diethyl ether and dried to constant weight. The materials were then suspended in water and ground by impact grinding to a particle size smaller than 0.2 mm; the finest particles were eliminated by repeated decantation in water. Elemental analyses (C, H, N) of the samples were carried out by means of a Carlo Erba 1106 analyzer.

ISEC Measurements. Full details on the sample preparations and on the chromatographic runs are given elsewhere.[6,16] Deuterium oxide, sugars, and polydestrans were employed as standard solutes when water was used as the mobile phase, whereas linear C_3-C_{30} hydrocarbons and linear polystyrenes were used in DCM and THF.

ESR Measurements. About 0.25 g of ground material was swollen with nitrogen-saturated 10^{-4} M solution of TEMPONE. The samples were allowed to reach swelling equilibrium, the excess solution was removed by pouring the so-obtained suspension onto filter paper, and then the swollen material was rapidly transferred into the ESR tube. The ESR spectra were recorded at 298 K on an X-band JEOL JES−RE1X apparatus at 9.4 GHz (modulation 100 kHz). The rotational correlation times τ were calculated according to the formula[17]

$$\tau = 1.75 \cdot 10^{-9} \cdot [1 - (h_{-1}/h_{+1})^{1/2}] \cdot \mathrm{DH}_{+1} \qquad (10)$$

The parameters h_{-1}, h_{+1} (amplitudes of the low- and high-field spectral lines, respectively) and DH_{+1} (width of the low-field spectral line) were obtained directly from the derivative spectrum by peak-picking. The numerical constant was estimated on the basis of published values for the anisotropic g and A tensors for TEMPONE.[18] Estimated precisions are given in the relevant figures.

PGSE−NMR Measurements. The self-diffusion coefficients of the swelling solvents were determined by ^{1}H PGSE−NMR measurements.[19] In this technique a spin-echo experiment is performed while two magnetic field gradient pulses of magnitude G, duration δ, and separation Δ are applied during the dephasing and the rephasing period, respectively. In the present study the interval Δ between the magnetic field gradient pulses was kept constant and equal to the interval t between the 90−180° radio frequency pulses. In these conditions, for nucleus with diffusion coefficient D, the height of the echo amplitude A is given by:

$$A = A_0 \exp[-2t/T_2 - \gamma^2 G^2 D \delta^2 (\Delta - \delta/3)] \qquad (11)$$

where γ is the magnetogiric ratio and T_2 is the spin-spin relaxation time of the nucleus. In the typical experiment A was measured at $\Delta = 10$ ms and $G = 58.0$ G/cm by varying δ up to 5 ms. The gradient strength was calibrated to values of the self-diffusion coefficient of pure water. The chosen t value was sufficient to remove the polymer contribution from the echo signal due to the relatively short T_2 relaxation time of the polymer hydrogens. The solvent diffusion coefficient was obtained from the slope of the logarithmic plot of A vs the term $\delta^2(\Delta - \delta/3)$. The samples were prepared as described above after swelling in the appropriate solvent and then placed in a 5 mm NMR tube. The spectra were recorded on a Bruker SXP 4−100 MHz apparatus operating at 21 MHz for protons, over the temperature range 5−35 °C at 5° intervals. The temperature of the sample during the measurements was controlled by a variable temperature unit BRUKER−VT 100 to an accuracy of within ±0.25 °C. Estimated precisions are given in the relevant figures.

Conclusions

ISEC, ESR, and PGSE−NMR offer an integrated picture of the relationship between the morphology on the nanometer scale of moderately cross-linked swollen gel-type resins (ISEC) and

the rotational and translational dynamics of molecules dispersed inside their polymer network (ESR and PGSE−NMR). The quantitative correlation between the ISEC and ESR analysis described by us for the first time in water[11] is fully confirmed in THF and DCM, and ISEC data are seen to quantitatively correlate also with the PGSE−NMR data. These new observations support our multimethodological approach to the study of structure on the nanometer scale and solutes dynamics of swollen gel-type resins. However, the quantitative correlation between the network polymer chain concentration (nanoporosity) as provided by ISEC with the translational mobility as given by PGSE−NMR is not interpretable on the basis of a classic hydrodynamic description of molecular mobility and further investigation is required. In essence, the Stokes−Einstein approach to translational mobility does not appear totally adequate for the physicochemical correlation, but a further approach based on tortuosity effects[15] appears to be promising. Finally, the translational mobility of water, THF, and DCM as determined with PGSE−NMR and the rotational mobility of a paramagnetic probe dissolved in the confined solvents are also found to mutually quantitatively correlate. However, the correlation is again not interpretable on the basis of a pure newtonian picture of the translational and rotational molecular motion of the solvent and the solute, respectively, and the physicochemical model has to be perfected.

Acknowledgment. We thank Doctor Silvano Lora (Istituto F.R.A.E., C.N.R., Legnaro, Padova-Italy) for the preparation of resins **M2**−**M8** and Doctor Karel Jeřàbek (Institute Chemical Processes Fundamentals, Academy of Sciences of the Czech Republic, Prague, Czech Republic) for providing assistance to A.A.D. and L.G. during ISEC measurements. B.C. gratefully acknowledges a scholarship provided by the Alexander von Humboldt Foundation.

References and Notes

(1) Harland, C. E. *Ion Exchange*, 2nd ed.; The Royal Society of Chemistry: Letchworth, 1994.

(2) (a) Reinicker, R. A.; Gates, B. C. *AIChE J.* **1972**, *20*, 933. (b) Corain, B.; Jeàbek, K. *Chim. Ind. Milan* **1996**, *78*, 563.

(3) (a) *Industrial Application of Immobilized Biocatalysts*; Tanaka, A., Tosa, T., Kobayashi, T., Eds.; Marcel Dekker, Inc.: New York, 1993. (b) Katchalski-Katzir, E. *TIBTECH* **1993**, *11*, 471. (c) Whitesides, G. M.; Wong, C. W. *Angew. Chem., Int. Ed. Engl.* **1985**, *24*, 617. (d) Yamada, H.; Shimizu, S. *Angew. Chem., Int. Ed. Engl.* **1988**, *27*, 622. (e) Wiseman, A. *J. Chem. Educ.* **1996**, *73*, 55.

(4) Arshady, R. *Adv. Mater.* **1991**, *3*, 182.

(5) (a) Guyot, A. In *Synthesis and Separations Using Functional Polymers*; Sherrington, D. C., Hodge, P., Eds.; John Wiley: New York, 1988; p 1. (b) Guyot, A. *Pure Appl. Chem.* **1988**, *60*, 365.

(6) Jeřàbek, K. *Anal. Chem.* **1985**, *57*, 1598.

(7) Nimtz, G. In *Correlations and Connectivity*, Stanley, H. E., Ostrowsky, N., Eds.; NATO ASI Series 118; Kluwer: Pordrecht, 1990; p 1.

(8) *Synthesis and separations using functional polymers*; Sherrington, D. C.; Hodge, P., Eds.; John Wiley: New York, 1988.

(9) Wagner, R.; Lange P. M. *Erdoel, Erdgas, Kohle* **1989**, *105*, 414.

(10) Corain, B.; D'Archivio, A. A.; Galantini, L.; Jeřàbek, K.; Králik, M.; Lora, S.; Palma, G.; Zecca, M. *Supported Reagents and Catalysts in Chemistry*; The Royal Society of Chemistry: Cambridge, in press.

(11) (a) Biffis, A.; Corain, B.; Zecca, M.; Corvaja, C.; Jeřàbek, K. *J. Am. Chem. Soc.* **1995**, *117*, 1603, and references therein. (b) Zecca, M.; Biffis, A.; Palma, G.; Lora, S.; Jeřàbek, K.; Corain, B. *Macromolecules* **1996**, *29*, 4655.

(12) (a) Stilbs, P. *Prog. NMR Spectrosc.* **1987**, *19*, 1, and references therein. (b) Pickup, S.; Blum, F. D.; Ford, W. T.; Periyasamy, M. *J. Am. Chem. Soc.* **1986**, *108*, 3987.

(13) Ogston, A. G. *Trans. Faraday Soc.* **1958**, *54*, 1754.

(14) Watanabe, T.; Yahagi, T.; Fujiwara, S. J. *J. Am. Chem. Soc.* **1980**, *102*, 5187.

(15) Mackie, J. S.; Meares, P. *Proc. R. Soc. London, Ser. A* **1955**, *232*, 498.

(16) Jeřàbek, K.; Setinek, K. *Polym. Sci., Part A: Polym. Chem.* **1990**, *28*, 1387.

(17) Bailey, P.; Gillies, D. G.; Sutcliffe, L. H. *J. Chem. Soc., Faraday Trans.* **1990**, *86*, 3309.

(18) Brustolon, M.; Maniero, A. L.; Corvaja, C. *Mol. Phys.* **1984**, *51*, 1269.

(19) Stejskal, E. O.; Tanner, J. E. *J. Chem. Phys.* **1965**, *42*, 288.